ELSEVIER

Thermochimica Acta 372 (2001) 67–74

thermochimica acta

www.elsevier.com/locate/tca

Thermal and devitrification behavior of $(2.5 - x)CaO{\cdot}(x/3)In_2O_3{\cdot}2SiO_2$ glasses

A. Costantini*, G. Luciani, F. Branda

Dipartimento di Ingegneria dei Materiali e della Produzione, Universita Federico II di Napoli, Piazzale Tecchio, 80125 Napoli, Italy

Received 15 May 2000; received in revised form 19 October 2000; accepted 20 December 2000

Abstract

A study of the influence of the substitution of In_2O_3 for CaO at constant O/Si ratio on thermal properties and non-isothermal devitrification of $2.5CaO{\cdot}2SiO_2$ is reported. Differential thermal analysis (DTA) and X-ray diffraction analysis were used.

The X-ray diffraction pattern of the crystallized In_2O_3 base glass shows that the α-$CaO{\cdot}SiO_2$, that should be stable only above 1125°C, forms in the temperature range 900–1000°C.

A new ternary crystalline phase whose reflections are not reported in the JCPDS cards, was found to form during crystallization of the glass. As their intensity progressively increases with substitution, they should refer to a In_2O_3 rich phase.

The glass transformation temperature T_g results can be explained on the basis of the increased structural rigidity when Ca^{2+} ions are substituted by In^{3+} with the formation of stronger bond to the oxygen, while crystal growth activation energy (E_c) values can be explained considering the increasing of the crystallization temperature T_p.

Devitrification involves a mechanism of surface nucleation; surface nuclei behaving as bulk nuclei in samples that soften and sinter before devitryfing.

Keywords: Glass structure; Glass transformation temperature; Non-isothermal crystallization; Substituted (In) calcium silicates

1. Introduction

In this paper, the study of the thermal properties and of the devitrification behavior of glasses of the system $CaO–In_2O_3–SiO_2$ is reported. The effect of the substitution of In_2O_3 to CaO in the composition of the glass $2.5CaO{\cdot}2SiO_2$ was studied. The substitution is such that not to change the O/Si ratio.

It is worth remembering that well-known bioactive glasses have CaO and SiO_2 as major components in the molar ratio $CaO/SiO_2 \cong 1$ [1,2].

Recently, it was found [3–5] that non-isothermal devitrification of glasses of composition $CaO–La_2O_3$ (MgO)–SiO_2 has peculiar characteristics. They devitrify through a surface nucleation mechanism. However, since in the temperature range of efficient crystal growth, softening and sintering occur, surface nuclei behave virtually as bulk nuclei. This was well supported by SEM observations of samples devitrified during a DSC run [5].

2. Experimental

Glasses of composition expressed by the following formula

$$(2.5 - x)CaO \cdot (x/3)ln_2O_3 \cdot 2SiO_2$$

* Corresponding author. Tel.: +39-81-768-2596; fax: +39-81-768-2413.
E-mail address: anicosta@unina.it (A. Costantini).

0040-6031/01/$ – see front matter
PII: S0040-6031(01)00435-X

were prepared by melting analytical grade reagents, In_2O_3, $CaCO_3$ and SiO_2 in a platinum crucible in an electric furnace for 4 h in the temperature range 1400–1600°C. The melts were quenched by plunging the bottom of the crucible into cold water.

Differential thermal analysis (DTA) was carried out by means of a Netzsch differential scanning calorimeter (DSC) model 404M on about 50 mg powdered samples at various heating rates (2–20°C min^{-1}). Finely (63–90 μm) and coarsely (315–500 μm) powdered samples were used. Powdered Al_2O_3 was used as reference material.

Devitrified samples were analyzed by computer-interfaced X-ray (Cu Kα) powder diffractometry (XRD) using a Philips Diffractometer model PW1710, with a scan speed of 1° min^{-1} and a built-in computer search program. The crystalline phases were identified by means of JCPDS cards.

3. Results

Figs. 1 and 2 show the DTA curves obtained for finely and coarsely powdered samples, respectively. All curves show a slope change just after the glass transition temperature. It is due to softening and sintering of the sample and the consequent variation of the heat transfer coefficient as the sample holder-sample contact changes. As a matter of fact, in these cases, the initially powdered samples were recovered from the sample holder as, more or less porous, sintered bodies. The softening effect is more pronounced in the case of fine powders and in samples with higher In_2O_3 content. The glass transformation temperature (T_g) was taken as the maximum of the DDTA curve recorded at 10°C min^{-1} (not reported) in the glass transformation range. DTA exothermic peak temperature (T_p) was taken as the minimum of crystallization peak. Their values are plotted in Fig. 3 versus the glass composition expressed as the x-values in the general formula of the series. As can be seen increasing trends for T_g and T_p are observed.

Fig. 4 shows the X-ray diffraction patterns of the samples submitted to a DTA run stopped just after the exothermic peak. The lines were attributed by means of the JCPDS cards. In all patterns, the lines of wollastonite (JCPDS card 27/88) appear. In the (a) pattern ($x = 0$), the lines of pseudo-wollastonite, α-$CaO{\cdot}SiO_2$ (JCPDS card 19/248) and $3CaO{\cdot}SiO_2$ (JCPDS card 11–593) are also present. It is interesting to observe that α-$CaO{\cdot}SiO_2$ is the high temperature phase, that in the binary $CaO{\cdot}SiO_2$ phase diagram, is reported to be stable above 1125°C. In the ((b), (c) and (d)) patterns, other lines appear that could not be identified by means of JCPDS cards. Non-isothermal devitrification was also studied. The kinetic

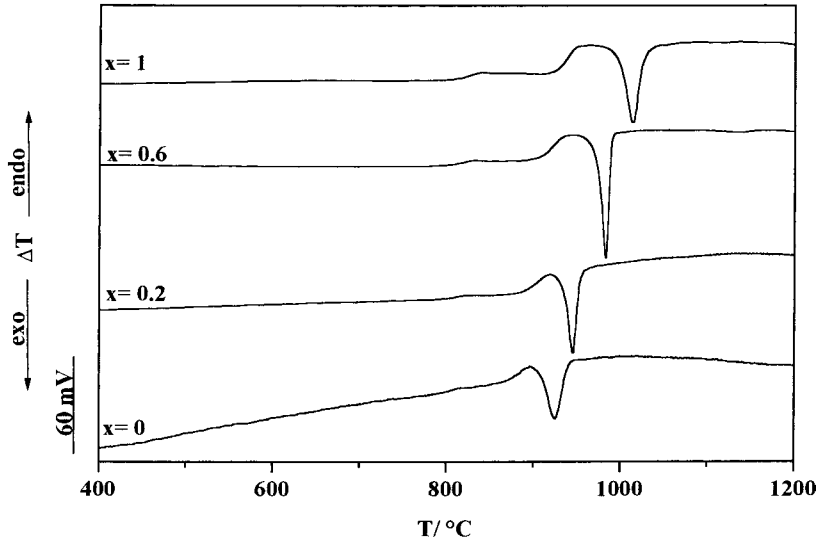

Fig. 1. DTA curves recorded at 10°C min^{-1} on finely (63–90 μm) powdered samples.

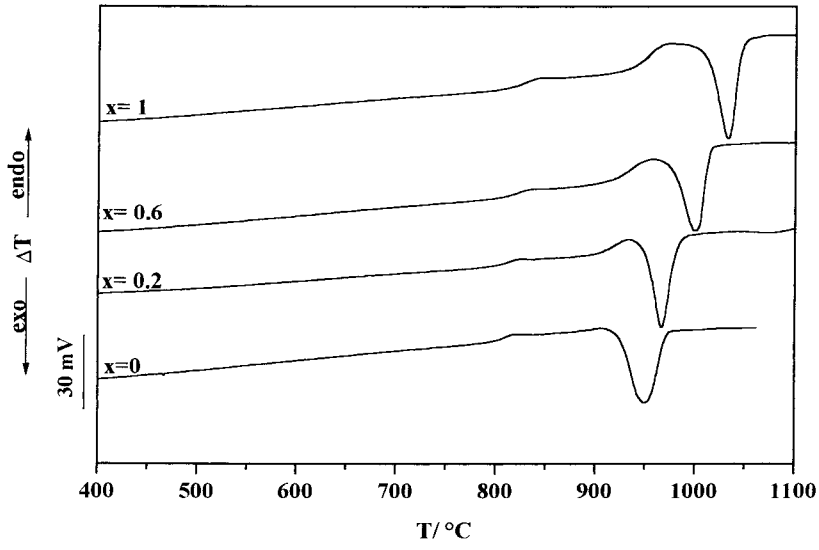

Fig. 2. DTA curves recorded at 10°C min^{-1} on coarsely (315–500 μm) powdered samples.

parameters were determined using the two following equations:

$$\ln \beta = \frac{-E_c}{RT_p} + \text{const} \quad (1)$$

$$\ln \Delta T = \frac{-mE_c}{RT} + \text{const} \quad (2)$$

that can be derived from the well-known following one [6,7]:

$$-\ln(1-\alpha) = \left(\frac{AN}{\beta^m}\right)\exp\left(\frac{-mE_c}{RT}\right) \quad (3)$$

where α is the crystallization degree, N the nuclei number, A a constant, β the heating rate, ΔT and T_p

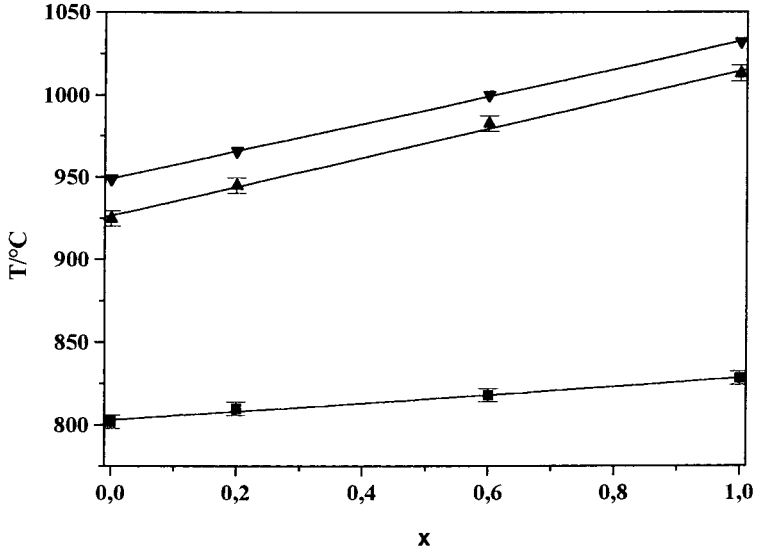

Fig. 3. T_g (■), and T_p for finely (▲) and coarsely powdered (▼) samples vs. composition (x) (from the DTA curve recorded at 10°C min^{-1}).

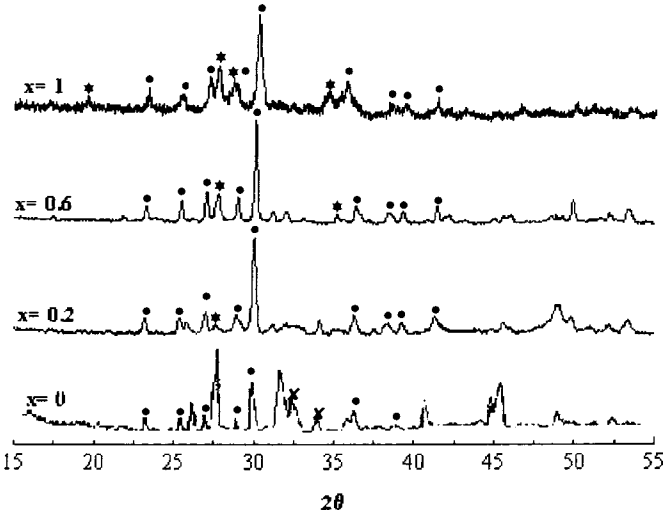

Fig. 4. X-ray diffraction patterns of samples devitrified during a DTA run: (●) wollastonite; (○) pseudo-wollastonite; (■) $3CaO{\cdot}SiO_2$; (◆) unknown phase.

the deflection from the baseline and the peak temperature. Since in silicate glasses, the devitrification exo-peak occurs in a higher temperature range than efficient nucleation [6], E_c is the crystal growth activation energy. The parameter m depends on the mechanism and morphology of crystal growth; it ranges from $m = 1$ for one-dimensional growth to $m = 3$ for three-dimensional growth [6,7].

Eqs. (1) and (2) can be derived from Eq. (3) by supposing that: (1) the value of α at peak temperature is not dependent on the heating rate [8]; (2) ΔT is proportional to the instantaneous reaction rate [9,10]; (3) in the initial part of the DTA crystallization peak,

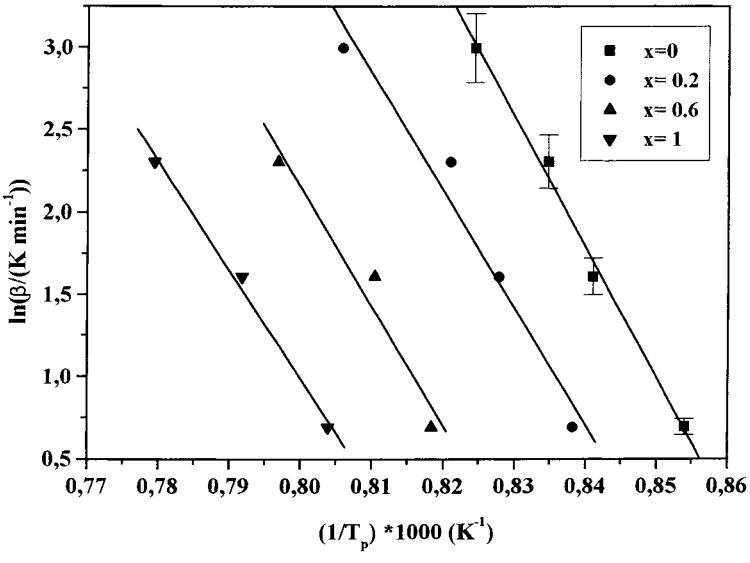

Fig. 5. The ln β vs. $1/T_p$ curve for finely powdered (63–90 μm) samples.

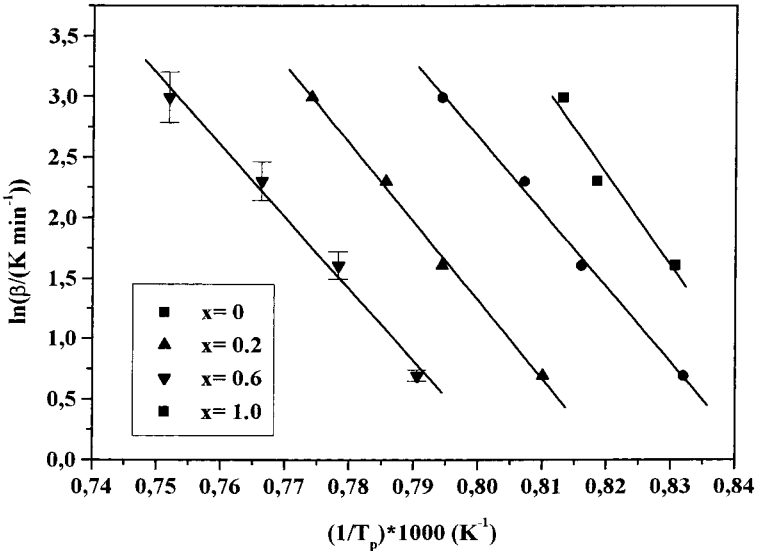

Fig. 6. The ln β vs. $1/T_p$ curve for coarsely powdered (315–500 μm) samples.

the change in the temperature has a much greater effect on ΔT than α [11].

In Figs. 5 and 6, the plot of ln β versus $1/T_p$ is reported for finely and coarsely powdered samples, respectively. The error committed is based on what reported in literature [12,18]. In Figs. 7 and 8, the plots of ln ΔT versus $1/T$ are reported for finely and coarsely powdered samples. They were calculated on the DTA curve recorded at 10°C min^{-1}. According to Eqs. (1) and (2) straight lines were obtained. Their slopes allow the determination of values of E_c and mE_c and, therefore, m for each glass. In Table 1, E_c and mE_c values, respectively, are reported as a function of the composition. A decreasing trend of E_c values is obtained as x

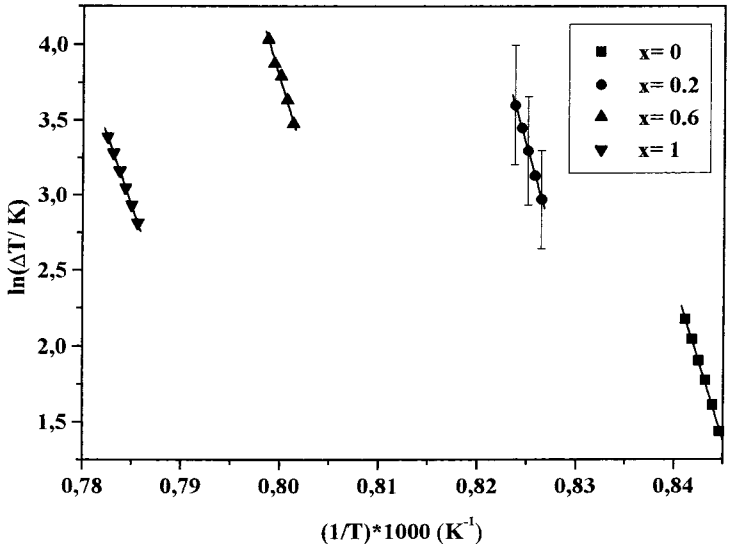

Fig. 7. The ln ΔT vs. $1/T$ curves for finely powdered (63–90 μm) samples (from the DTA curve recorded at 10°C min^{-1}).

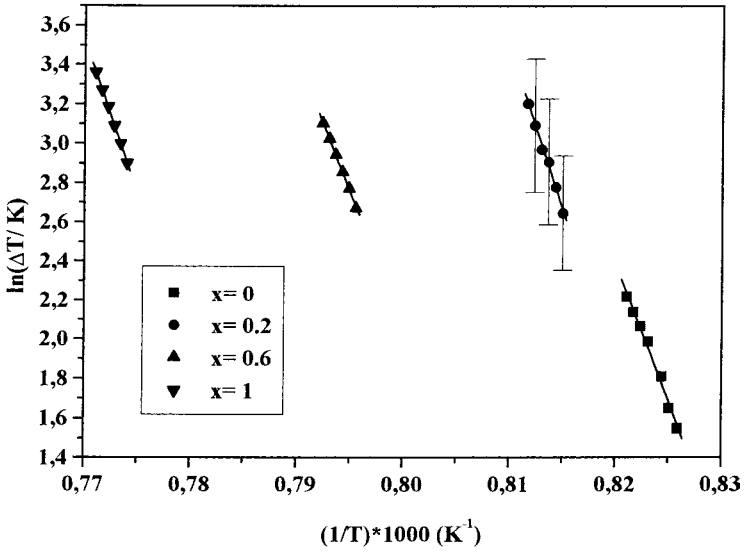

Fig. 8. The ln ΔT vs. $1/T$ curves for coarsely powdered (315–500 μm) samples (from the DTA curve recorded at 10°C min^{-1}).

Table 1
E_c and mE_c values for finely and coarsely powdered samples

x	E_c (kJ mol^{-1})	mE_c (kJ mol^{-1})	
		Fine	Coarse
0	665 ± 34	1724 ± 172	1163 ± 115
0.2	595 ± 30	1941 ± 190	1364 ± 136
0.6	605 ± 30	1941 ± 190	1138 ± 114
1	551 ± 27	1573 ± 160	1280 ± 128

increases. It is interesting to observe that the m-values relative to finely powdered samples are greater than the ones relative to coarsely powdered samples.

4. Discussion

The role of SiO_2 and CaO in the glass structure are well known: the former is a network former oxide, while the latter is a network modifier. In_2O_3 is a less common component of glasses. The criterion reported in the literature [13,19] suggest that it is expected to be a network modifier. T_g versus composition curves of glasses of the system Na_2O–M_2O_3–SiO_2 (M = La, Sc, Y, Al, B) proved to be linked to the nature of former/modifier of the substituting oxide [17].

Following Ray [16], T_g values depend on the density of covalent cross-linking between the oxygens and the cations. In the studied series, the ratio O/Si is constant, therefore, no change in the covalent cross-linking density occurs. Hence, in this case any differences in T_g values must be attributed to changes of the numbers and strengths of cross-linking of the network modifier cations. The increasing trend of T_g values could be attributed to the substitution of In^{3+} to Ca^{2+} ions. In fact, both are modifier cations, the former having a much greater field strength ($Z/r^2 = 4.57$ $Å^{-2}$ instead of 2.04 $Å^{-2}$) but a lower coordination number (6 instead of 8). However, the increasing strength of the cross-links prevails on their number and make T_g increase. Whereas, T_g depends on the structure of the glasses, T_P depends on the kinetic parameters of the devitrification process. These glasses show a surface nucleation and the number of surface nuclei in fine samples is greater than in the course ones. Therefore, different values of the peak temperature (T_p) were obtained for finely and coarsely powdered samples.

It worth remembering that E_c is usually equal to the viscous flow activation energy E_η [14,18]. Moreover, the viscosity and the viscous flow activation energy decrease with temperature according to the Vogel–Fulcher–Tamman equation [15]. Although the struc-

ture rigidity increases with substitution of In_2O_3 to CaO, the shift of crystallization to higher temperatures makes E_η and, therefore, E_c decrease.

Since E_c has similar values for finely and coarsely powdered samples, while mE_c data are higher for the latter, the m-values appear to increase as the specific surface is increased (Table 1). Usually [20], the opposite result is obtained owing to the fact that the greater the specific surface the greater the tendency to devitrify by growth from surface nuclei, so that m progressively reduces to 1. In the case of diopside glass [21] and glasses of composition $CaO{\cdot}SiO_2$, $1.6CaO{\cdot}0.4MgO{\cdot}2SiO_2$ and $1.4CaO{\cdot}(0.6/3)Y_2O_3{\cdot}2SiO_2$ [3–5], it was found that nucleation preferentially occurs at the surface of the sample, but surface nuclei formed in the glass transformation temperature range behave as bulk nuclei in finely powdered samples that efficiently sinter before devitrifying. This hypothesis appears to be effective in explaining the devitrification behavior of the studied glasses. In fact, lower m-values were obtained for coarsely powdered samples that badly sinter.

The XRD pattern of the devitrified base glass shows that the α-$CaO{\cdot}SiO_2$ forms in the temperature range 900–1000°C, while it should be stable only above 1125°C. A new ternary crystalline phase whose reflections are not reported in the JCPDS cards was found to form during crystallization of the glass. As their intensity progressively increases with substitution, they should refer to a In_2O_3 rich phase.

5. Conclusions

1. The XRD pattern of the devitrified base glass shows that the α-$CaO{\cdot}SiO_2$ forms in the temperature range 900–1000°C, while it should be stable only above 1125°C. A new ternary crystalline phase whose reflections are not reported in the JCPDS cards, was found to form during crystallization of the glass. As their intensity progressively increases with substitution, they should refer to a In_2O_3 rich phase.
2. T_g increase as In_2O_3 is substituted to CaO. This is the result of the substitution between two modifying cations: Ca^{2+} and In^{3+}, the latter having a lower coordination number but a much greater ionic field strength.
3. E_c decreases with substitution; this is the consequence of the shift of crystallization to a higher temperature range.
4. Devitrification involves a mechanism of surface nucleation; in samples that soften and sinter before devitryfing surface nuclei behave as bulk nuclei.

References

[1] L.L. Hench, Bioceramics: from concept to clinic, J. Am. Ceram. Soc. 74 (7) (1991) 1487–1510.

[2] T. Kokubo, Novel bioactive materials derived from glasses, in: Proceedings of the XVII International Congress on Glass, Vol. 1, Madrid, Bol. Soc. Esp. Ceram. Vid. 31+C1 (1992) 119–137.

[3] A. Costantini, R. Fresa, A. Buri, F. Branda, Thermal properties and devitrification behaviour of $(2-x)CaO{\cdot}(x/3)La_2O_3{\cdot}2SiO_2$, Silicates Ind. 7/8 (1996) 171–175.

[4] A. Costantini, F. Branda, A. Buri, Thermal properties and devitrification behaviour of $(1+x)CaO{\cdot}(1-x)MgO{\cdot}2SiO_2$, J. Mater. Science 30 (1995) 1561–1564.

[5] F. Branda, A. Costantini, A. Buri, A. Tomasi, Devitrification behaviour of $CaO–MgO(Y_2O_3)–SiO_2$ glasses, J. Thermal Anal. 41 (1994) 1479–1487.

[6] K. Matusita, S. Sakka, Kinetic study of non-isothermal cystallisation of glass by thermal analysis, Bull. Inst. Chem. Res. Kyoto Univ. 59 (1981) 159–171.

[7] D.R. MacFarlane, M. Matecki, M. Poulanin, Crystallization in fluoride glasses devitrification on re-heating, J. Non-Cryst. Solids 64 (1984) 351–362.

[8] P.G. Boswell, On the calculation of activation energies using a modified Kissinger method, J. Thermal Anal. 18 (1980) 353–358.

[9] H.J. Borchardt, F. Daniels, The application of differential thermal analysis to the study of reaction kinetics, J. Am. Chem. Soc. 79 (1957) 41–46.

[10] K. Akita, M. Kase, Relationship between the DTA peak and the maximum reaction rate, J. Phys. Chem. 72 (1968) 903–913.

[11] F.O. Piloyan, I.V. Ryabchica, O.S. Novikova, Determination of activation energies of chemical reactions by differential thermal analysis, Nature 212 (1996) 1229.

[12] J. Sestak, The applicability of DTA to the study of crystallisation kinetic of glasses, Phys. Chem. Glasses 15 (6) (1974).

[13] H. Rawson, Inorganic Glass Forming Systems, Academic Press, London, 1967, pp. 24–25.

[14] P.W. Mc Millan, Glass-Ceramics, Academic Press, New York, 1964.

[15] R.C. Weast, CRC Handbook of Chemistry and Physics, 58th Edition, CRC Press, Ohio, 1977–1978.

[16] N.H. Ray, Compositon-property relationship in inorganic oxide glasses, J. Non-Cryst. Solids 15 (1974) 423–434.

[17] F. Banda, F. Arcobello Varlese, A. Costantini, G. Luciani, T_g and FTIR of $(2.5 - x)CaO{\cdot}(x/3)M_2O_3{\cdot}2SiO_2$ (M = Y, La, In, Al, Ga) glasses, J. Non-Cryst. Solids 246 (1999) 27–33.
[18] K. Matusita, S. Sakka, Kinetic study on crystallisation of glass by differential thermal analysis — criterion on application of Kissinger plot, J. Non-Cryst. Solids 38/39 (1980) 741.
[19] H. Scholze (Ed.), Le Verre, Institut du Verre, Paris, 1980, p. 69.
[20] A. Marotta, A. Buri, F. Branda, Thermochim. Acta 40 (1980) 397–404.
[21] F. Branda, A. Costantini, A. Buri, Non-isothermal devitrification behaviour of diopside glass, Thermochim. Acta 217 (1993) 207–212.